# $Al^{III}$ Ion Complexes of Saccharic Acid and Mucic Acid: A Solution and Solid-State Study

**Andrea Lakatos,[a] Roberta Bertani,*[b] Tamas Kiss,*[a, c] Alfonso Venzo,[d] Maurizio Casarin,[e] Franco Benetollo,[f] Paolo Ganis,[d] and Donata Favretto[d]**

**Abstract:** The $Al^{III}$-binding abilities of two aldaric acids, D-saccharic acid and mucic acid (the neutral form is denoted as $H_2L$), were studied in solution by means of pH potentiometric, $^1H$ and $^{13}C$ NMR, and ESI-MS techniques. The most probable conformations and isomeric binding modes of the complexes formed in solution were determined by density functional theory (DFT) calculations. A solid D-saccharic acid complex $K_2[\{Al(LH_{-2})(H_2O)\}_2]\cdot H_2O$ was isolated and crystallographically characterised. The two alcoholic hydroxy groups α to the terminal $COO^-$ groups were found to take part in the coordination, but in different ways. One of them coordinates in a bridging mode. Detailed ESI-MS and NMR studies proved that the complex retains its structure in solution. However, depending on the ligand and the pH, such complexes may exist in two isomeric forms. DFT calculations on the ion $[\{Al(LH_{-2})(H_2O)\}_2]^{2-}$ revealed that several orbitals participate in stabilizing the dimeric arrangement.

**Keywords:** aluminum · carbohydrates · coordination modes · Density functional calculations · structure elucidation

## Introduction

The coordination chemistry of $Al^{III}$ ions with naturally-occurring ligands has broadened rapidly in recent years, because of its environmental and medical applications. Interest in the solution speciation of these systems is also increasing as such information could provide a basis for a better understanding of the distribution, transport, and toxicity of $Al^{III}$ ions both in the environment and in humans.[1] The involvement of $Al^{III}$ ions in Alzheimer's disease is still a controversial issue.[2]

$Al^{III}$, as a typical hard-metal ion, prefers the coordination of oxygen donors, especially negatively-charged ones, such as carboxylates, phenolates, alcoholates, and phosphates.[3] (Poly)hydroxy(poly)carboxylates, including citric acid,[4,5] tartaric acid,[6,7] gluconic acid[8] and sugar carboxylates,[8–10] are strong $Al^{III}$ ion binders that are able to prevent the hydrolysis of the metal ion under physiological conditions. $Al^{III}$ ions have a strong tendency to promote deprotonation of weakly acidic alcoholic OH groups in hydroxycarboxylic acids,[3] even in the acidic pH range. Indeed, this is how $Al^{III}$ ions form stable complexes with this ligand group. Polydentate coordination of such ligands results in the formation of oligonuclear complexes in which alcoholate and carboxylate oxygen atoms can behave as bridging donors. For example, under thermodynamic equilibrium conditions citrate forms trinuclear complexes over a wide pH range.[5] Tartaric acid (ta), which is a C4 aldaric acid, has been found to form predominantly dinuclear complexes in various protonation states ($[Al_2(taH_n)_2]$ $n=0$ to $-2$) in the pH range 3.5–7.[6] In the fully deprotonated complex $[Al_2(taH_{-2})_2]^{2-}$, the metal ions are bridged by two quadridentate (4−) ligands in a 4× ($COO^-$,$O^-$) binding mode, but the $O^-$ moieties undergo gradual protonation. The binding mode of the dimeric spe-

[a] Dr. A. Lakatos, Prof. Dr. T. Kiss
Biocoordination Chemistry Research Group
of the Hungarian Academy of Sciences
University of Szeged, P.O. Box 440, 6701 Szeged (Hungary)
Fax: (+36) 62-544-337
E-mail: tkiss@chem.u-szeged.hu

[b] Prof. Dr. R. Bertani
Department of Chemical Processes of Engineering
University of Padova and Institute of Molecular Sciences CNR
Via F. Marzolo 9, Padova (Italy)
E-mail: roberta.bertani@unipd.it

[c] Prof. Dr. T. Kiss
Department of Inorganic and Analytical Chemistry
University of Szeged, P.O. Box 440, 6701 Szeged (Hungary)
E-mail: tkiss@chem.u-szeged.hu

[d] Dr. A. Venzo, Prof. Dr. P. Ganis, Dr. D. Favretto
Institute of Molecular Science and Technology
CNR, Via F. Marzolo 1, Padova (Italy)

[e] Prof. Dr. M. Casarin
Department of Inorganic, Metalorganic and Analytical Chemistry
University of Padova, Via F. Marzolo 1, Padova (Italy)

[f] Dr. F. Benetollo
ICTIMA, CNR
Corso Stati Uniti 4, Padova (Italy)

Supporting information for this article is available on the WWW under http://www.chemeurj.org/ or from the author.

 **DOI: 10.1002/chem.200305328**  

cies has been confirmed by multinuclear NMR studies.[6] Interestingly, the mononuclear tris complex $[Al(taH_{-2})_3]^{9-}$ has also been detected by NMR spectroscopy in the basic pH range, but was not observed by pH potentiometry. The noteworthy stability and symmetry of this complex has been ascribed to the formation of successive hydrogen bonds through the remaining protonated hydroxy groups of each ligand molecule.[6]

The complexation of C6 aldaric acids with $Al^{III}$ ions has received relatively little attention. In an early potentiometric work[8] only the occurrence of mononuclear complexes was

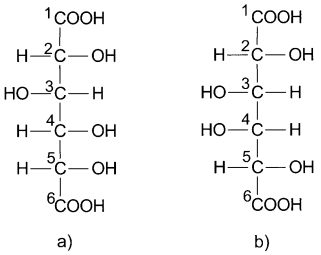


Figure 1. Open chain forms of the ligands in which the carbon atoms are numbered: a) D-saccharic acid and b) mucic acid.

considered for the $Al^{III}$/glucaric (D-saccharic) acid (see Figure 1a) system. More recently, Venema et al.[9] detected similar predominant dimeric complexes to those discussed above in the mixed metal-ion system $Al^{III}$–glucarate–$Ca^{II}$. In this complex the negatively charged carboxylate and alcoholate O-donors participate in the binding, and some of the alcoholates behave as bridging donors between the $Al^{III}$ and $Ca^{II}$ centres. To the best of our knowledge, metal complexation reactions of galactaric (mucic) acid (see Figure 1b), another C6 aldaric acid isomer, have not been reported so far.

The aim of the present work was to clarify the solution speciation and structure of complexes formed in the $Al^{III}$/saccharic and $Al^{III}$/mucic acid systems through the use of pH potentiometry, multinuclear NMR spectroscopy and ESI-MS spectrometry. Moreover, as it was isolated in the solid state, the X-ray structure of $K_2[Al_2(C_6H_6O_8)_2(H_2O)_2]\cdot H_2O$ was determined. Finally, further insight was obtained into the charge distribution and metal–ligand interactions of $[Al_2(C_6H_6O_8)_2(H_2O)_2]^{2-}$ by running density functional quantum mechanical calculations. The present detailed studies may provide general information on the versatile binding properties of the alcoholic OH/$O^-$ group in sugar derivatives through the formation of mononuclear and dinuclear complexes that involve coordination isomers.

## Results and Discussion

**Potentiometric results**: Potentiometric titrations of the ligands indicate the existence of overlapping stepwise deprotonations of two acidic protons from the two carboxylic groups of each ligand. The protonation constants are listed in Table 1. If the rather large differences in the experimental conditions (the ionic strength and the type of electrolyte used) are taken into account, these values are in fairly good agreement with those reported in the literature: 3.96 and 3.18 at 25 °C and 0.1 M $KNO_3$,[11] and 4.1 and 3.14 at 25 °C and 1.0 M $KNO_3$[8] for saccharic acid; and 3.63 and 3.08 at 25 °C and 1.0 M $NaNO_3$[12] for mucic acid.

Table 1. Stability constants for proton [$\log K$] and $Al^{III}$ ion complexes [$\log\beta$] of saccharic acid and mucic acid at 25 °C and $I = 0.2$ M (KCl).

| | $\log K/\log\beta$ | |
|---|---|---|
| Species | Saccharic acid | Mucic acid |
| $K([HL]^-)$ | 3.93(2) | 3.91(2) |
| $K([H_2L])$ | 3.07(2) | 3.06(3) |
| $[AlLH]^{2+}$ | 6.24(10) | 6.01(10) |
| $[AlL]^+$ | 3.45(5) | 3.36(7) |
| $[AlLH_{-3}]^{2-}$ | −11.05(2) | −11.20(2) |
| $[Al_2L_2H_{-2}]$ | 4.97(3) | 3.14(12) |
| $[Al_2L_2H_{-3}]^-$ | 2.11(2) | 0.02(8) |
| $[Al_2L_2H_{-4}]^{2-}$ | −1.94(2) | −3.42(2) |
| fitting [$\Delta cm^3$][a] | 0.0102 | 0.00670 |
| no. of points | 363 | 282 |

[a] The average difference between the experimental and the calculated titration curves expressed in the volume of the titrant.

The $Al^{III}$–ligand titration data were evaluated on the basis of literature results. As mentioned above, Motekaitis and Martell[8] assumed a very simple complexation model for the $Al^{III}$/saccharic acid system. They proposed a mononuclear 1:1 species of $[AlLH_{-1}]$ and $[Al(LH_{-2})]^-$. When this assumption was used in our calculations, a rather poor fit was obtained between the experimental and the calculated titration curves in both systems. In a potentiometric investigation of the $Al^{III}$-binding capabilities of tartaric acid (a ligand with similar coordination possibilities to those of saccharic and mucic acid), Marklund and Öhman[7] demonstrated the formation of dinuclear complexes. When their speciation model was adopted to our systems, the fitting parameter improved by one order of magnitude in comparison with the mononuclear model. The sharp increase in the titration curve at around pH 6 indicates that a species with stoichiometry $[AlLH_{-2}]_n$ is predominantly formed. Formation of 2:2 $Al^{III}$–ligand complexes has also been demonstrated in an aqueous solution of $Al^{III}$ ions, $Ca^{II}$ ions, and saccharic acid. Here the dimeric $Al^{III}$/saccharic acid complex binds one or two $Ca^{II}$ ions.[9] These results and observations suggest that a model that includes dinuclear complexes could give the correct speciation for these systems. The best fit between the experimental and the calculated titration curves was obtained when the species and stability constants listed in Table 1 were used. The species distributions for the complexes formed in the two systems as a function of pH are depicted in Figures 2 and 3. The most characteristic species in both systems is the dimeric complex $[Al_2L_2H_{-4}]^{2-}$; this is formed in the slightly acidic and neutral pH range. In the $Al^{III}$/mucic acid system under more acidic conditions (pH 3.8), in which $Al^{3+}$ is a dominant species, the protonated species $[Al_2L_2H_{-3}]^{2-}$ also exists in a rather small amount. On the other hand, there is a well defined equilibrium between the $Al^{III}$ ion and saccharic acid in the same pH range; this results in the formation of $[Al_2L_2H_{-4}]^{2-}$, as evidenced by NMR spectroscopy. Decomposition of the dimer $[Al_2L_2H_{-4}]^{2-}$ occurs in basic solutions to furnish the mono-

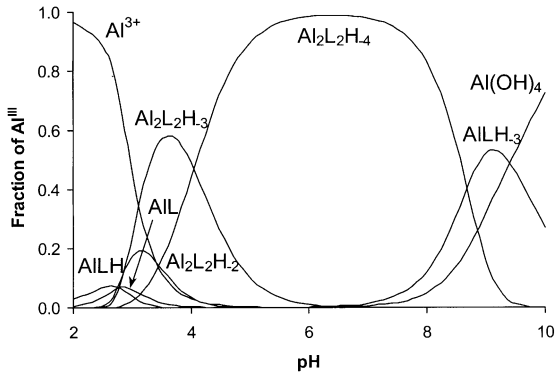


Figure 2. Species distribution curves as a function of pH in the $Al^{III}$/saccharic acid system at a ratio of 1:1, $c_{Al} = 0.002$ M.

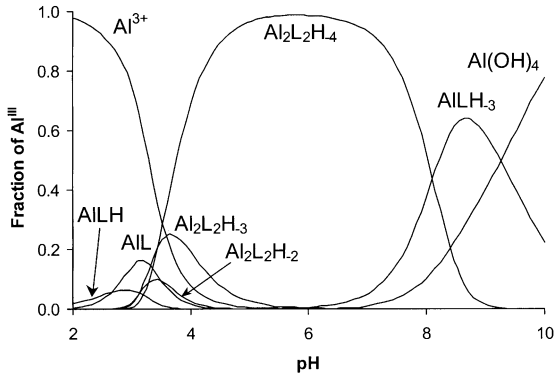


Figure 3. Species distribution curves as a function of pH in the $Al^{III}$/mucic acid system at a ratio of 1:1, $c_{Al} = 0.002$ M.

nuclear complex $[AlLH_{-3}]^{2-}$; this is most probably a mixed hydroxo species. Accordingly, further investigations were primarily focused on characterisation of the predominating dimeric complex $[Al_2L_2H_{-4}]^{2-}$.

## NMR spectroscopic studies

*$Al^{III}$/saccharic acid*: The $^1$H NMR spectrum of saccharic acid at pH 5.5 exhibits four multiplets: two doublets for H2 and H5, and two doublet of doublets for the H3 and H4 methine protons. The accurate assignment of the signals is based on the results of Van Duin et al.,[13] who used [2-$^2$H]saccharic acid. The chemical shift values and coupling constants measured at pH 5.5 are listed in Table 2.

The six carbon resonances for the ligand were assigned by two- dimensional H–C correlation measurements (see Table 2). Both the $^1$H and $^{13}$C NMR signals display considerable upfield shifts as pH increases. This is due to deprotonation of the carboxylic acid functions.

The $^1$H and $^{13}$C NMR spectra recorded between pH 5.5 and 7.5 of a sample that contains $Al^{III}$ ions and saccharic acid (0.08 M) in a molar ratio of 1:1 indicates the presence of a single species (denoted B); this is in close agreement with the potentiometric data (cf. Figures 2 and 4d). However,

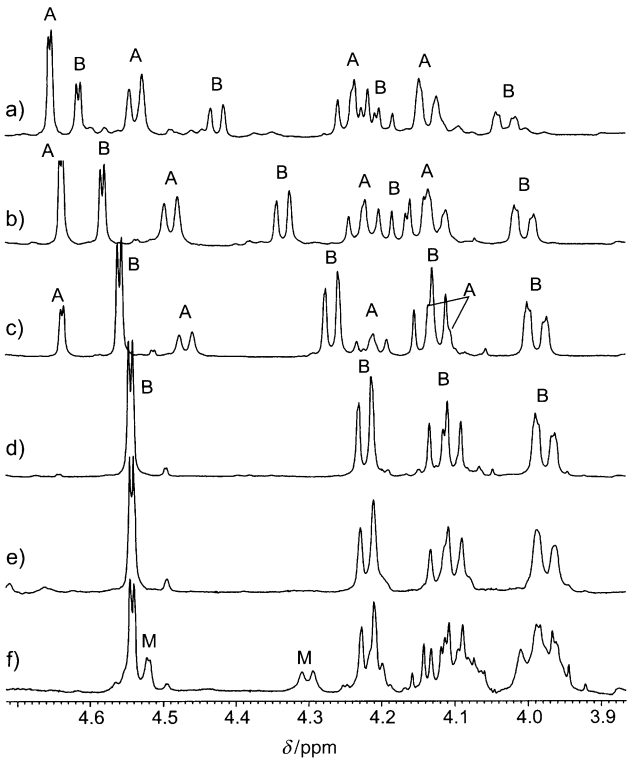


Figure 4. $^1$H NMR spectra obtained for the $Al^{III}$/saccharic acid system at a ratio of 1:1 and at pH values of: a) 2.5, b) 3.0, c) 4.0, d) 5.5, e) 6.1 and f) 7.5. A and B represent the two isomers observed for species $[Al_2L_2H_{-n}]$, while M represents species $[AlLH_{-3}]$ (see text).

Table 2. Characteristic NMR parameters in aqueous solution at 25 °C for free saccharic and mucic acid and their complex $[Al_2L_2H_{-4}]^{2-}$.

| Sample | $^1$H chemical shifts [ppm] | | | | $J_{(H,H)}$ [Hz] | | | |
|---|---|---|---|---|---|---|---|---|
| | H2 | H3 | H4 | H5 | $^3J_{(2,3)}$ | $^3J_{(3,4)}$ | $^3J_{(4,5)}$ | $^4J_{(2,4)}$ |
| saccharic acid pH 5.5 | | | | | | | | |
| free ligand | 4.159 | 4.081 | 3.948 | 4.137 | 3.05 | 4.64 | 4.65 | – |
| $[Al_2L_2H_{-4}]^{2-}$ | 4.222 | 4.112 | 3.977 | 4.543 | 3.67 | 4.65 | 0.98 | – |
| mucic acid pH 5.6 | | | | | | | | |
| free ligand | 4.265 | 3.957 | 3.957 | 4.265 | 0.11 | 0.66 | 0.11 | – |
| $[Al_2L_2H_{-4}]^{2-}$ (A) | 4.034 | 3.838 | 4.171 | 4.438 | 4.14 | 2.53 | 1.09 | 0.73 |
| $[Al_2L_2H_{-4}]^{2-}$ (B) | 4.039 | 3.893 | 4.248 | 4.419 | 4.15 | 2.45 | 0.98 | 0.76 |

| | $^{13}$C chemical shifts [ppm] | | | | | |
|---|---|---|---|---|---|---|
| | C1 | C2 | C3 | C4 | C5 | C6 |
| saccharic acid pH 5.5 | | | | | | |
| free ligand | 182.99 | 78.08 | 76.04 | 78.09 | 77.92 | 182.85 |
| $[Al_2L_2H_{-4}]^{2-}$ | 186.53 | 77.34 | 77.71 | 79.53 | 74.63 | 185.35 |
| mucic acid pH 5.6 | | | | | | |
| free ligand | 183.84 | 75.72 | 76.00 | 76.00 | 75.72 | 183.84 |
| $[Al_2L_2H_{-4}]^{2-}$ (A) | 187.42 | 77.27 | 80.95 | 79.96 | 77.10 | 184.50 |
| $[Al_2L_2H_{-4}]^{2-}$ (B) | 188.41 | 77.36 | 80.69 | 79.22 | 77.17 | 184.80 |

  

NMR spectroscopy does not provide direct evidence for the nuclearity of the complex. Other techniques such as ESI-MS and X-ray crystallography (vide infra) were used to unambiguously prove the formation of the dimeric species $[Al_2L_2H_{-4}]^{2-}$ in this pH range.

In the $^1$H NMR spectrum only four signals are observed. Clearly, this indicates that the two mononuclear moieties are magnetically equivalent. The shapes of the signals differ significantly from those observed for free saccharic acid at the same pH. In particular, there are large differences in the $^3J_{(H,H)}$ coupling constants. On the basis of the Karplus equation,[14] the geometric arrangement of saccharic acid must be modified substantially upon coordination with the $Al^{III}$ ion. The very low $^3J_{(H,H)}$ value between H4 and H5 (see Table 2) indicates a dihedral angle close to 90°; this suggests that the binding mode of the molecule is rather rigid. The same dihedral angle can be seen between the protons attached to C4 and C5 in the crystal structure of $[Al_2L_2H_{-4}]^{2-}$ (vide infra). Thus, the signal at 4.543 ppm was attributed to H5 and serves as the starting point for assignment of the signals made by means of two-dimensional measurements. (The $^1$H–$^{13}$C heterocorrelated spectrum recorded at pH 5.5 is depicted in Figure S1 in the Supporting Information.) The NMR parameters for species B are listed in Table 2. The considerable downfield shift of the H2 ($\Delta\delta = 0.063$ ppm) and H5 ($\Delta\delta = 0.406$ ppm) signals relative to those for the free ligand (see Table 2) suggests that apart from the two carboxylates (the $^{13}$C resonances of which are also shifted downfield considerably upon complexation), the 2- and 5-hydroxy groups may also be involved in the coordination of the $Al^{III}$ ion. A binding mode similar to that proposed by Venema et al.[5] for a 2:2 $Al^{III}$ ion complex of tartaric acid can also be expected in this system.

Table 3. Crystal data and experimental details for the X-ray diffraction study for compound $K_2[\{Al(C_6H_6O_8)(H_2O)\}_2]\cdot H_2O$.

| | |
|---|---|
| formula | $C_{12}H_{22}O_{19}K_2Al_2$ |
| $M_r$ | 602.45 |
| crystal system | orthorhombic |
| space group | $C222_1$ |
| $Z$ | 4 |
| $a$ [Å] | 10.723(3) |
| $b$ [Å] | 13.664(3) |
| $c$ [Å] | 13.186(3) |
| $V$ [Å$^3$] | 1932.0(8) |
| $\rho_{calcd}$ [g cm$^{-3}$] | 2.071 |
| $\mu$ [cm$^{-1}$] | 6.89 |
| $T$ [°C] | 23 |
| $R$ | 0.059[a] |
| $R_w$ | 0.150[b] |

[a] $R = \sigma||F_o| - |F_c||/\sigma|F_o|$. [b] Refinement on $F^2$ $wR_2 = \{\sigma[(F_o^2 - F_c^2)^2]/\sigma[w(F_o^2)^2]\}^{1/2}$.

When the pH is lowered from 5.5 to 2.5, the intensities of the resonances ascribed to the dimeric complex $[Al_2L_2H_{-4}]^{2-}$ decrease and a new set of signals with a similar arrangement and multiplicity appear at higher $\delta$ values (see Figure 4). The $^1$H–$^{13}$C heterocorrelated NMR spectrum for the 1:1 $Al^{III}$/saccharic acid system at pH 3 is given in Figure S2 in the Supporting Information. Moreover, a considerable downfield shift of both sets of signals, A and B (see Figure 4), is observed with decreasing pH. This means that both A and B are the weighted average resonances of the complexes, and that they experience a fast proton exchange. Thus, taking into account the potentiometric results, the set of signals for B, which exist in a wider pH range (pH 2–6), may be attributed to the dimeric complex $[Al_2L_2H_{-4}]^{2-}$ and its protonated forms $[Al_2L_2H_{-3}]^{-}$ and $[Al_2L_2H_{-2}]$. These last complexes have structures similar to that of $[Al_2L_2H_{-4}]^{2-}$, but one or more of the coordinated hydroxy groups are protonated. Assignment of the signals for A is not so unambiguous. There are two possibilities: 1) there is a monomer–dimer equilibrium and the new signals are those of the monomeric complexes or 2) a different coordination isomer of the protonated dimers is formed, one which is not favoured for some reason in the case of $[Al_2L_2H_{-4}]^{2-}$. As regards the first explanation, neither potentiometry nor ESI-MS (vide infra) support the formation of monomeric complexes at such a metal-ion concentration. Thus, we suggest that in a manner similar to that found in the $Al^{III}$/tartaric acid system, mainly dimeric species are formed and they exist as two coordination isomers. The shapes of the multiplets of the two isomers are similar; this suggests that the saccharic moieties have a similar geometric arrangement.

At pH > 7.5, when $OH^-$ starts to displace the complexed ligand from the coordination sphere of the metal ion, not only can the signals for $[Al_2L_2H_{-4}]^{2-}$ and the free ligand be observed, but new resonances (M) can also be detected in the $^1$H NMR spectra (Figure 4f). Our potentiometric results suggest that these signals may be due to the mononuclear species $[AlLH_{-3}]^{2-}$, which is most likely a mixed hydroxo complex with a ($COO^-$,$O^-$,$O^-$,$OH^-$) binding mode. Bis or tris complexes could not be detected either by potentiometry or by NMR spectroscopy, even at a ten-fold excess of ligand.

*$Al^{III}$/mucic acid*: The NMR spectra of mucic acid are simpler than those of saccharic acid, because of the symmetric structure of the ligand. Only two second-order triplets are present in the $^1$H NMR spectrum recorded at pH 5.6. The signal at 4.265 ppm was attributed to H2 and H5, because heteronuclear correlations to the adjacent carbonyl carbons could be detected only for these nuclei in the HMBC measurements. The complete assignment of the $^1$H and $^{13}$C parameters is listed in Table 2. On the basis of the Karplus equation,[14] the very small $^3J_{(H,H)}$ values observed suggest a molecular geometry in which the dihedral angles between the hydrogens are close to 90°.

Upon addition of $Al^{III}$ ions to a 0.07 M solution of the ligand in a ratio of 1:1.1 at pH 5.6, two sets of four signals are observed in both the $^1$H and $^{13}$C NMR spectra. They have similar shapes and an internal integration ratio of 65:35. A small quantity (ca. 6%) of free ligand is also observed. The ratio of the two species does not change appreciably in the pH range 4.5–7.5 (Figure 5). The shapes of the signals are quite different from those observed for the free ligand; this suggests that, as in the case of saccharic acid, substantial conformational changes are induced upon metal-ion coordination. As evidenced from the COSY, NOESY

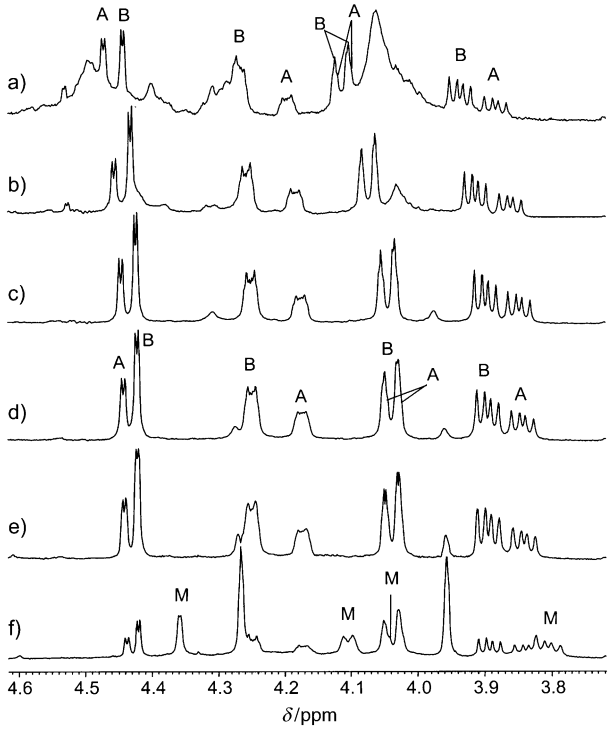


Figure 5. $^1$H NMR spectra obtained for the $Al^{III}$/mucic acid system at a ratio of 1:1 and at pH values of: a) 2.6, b) 3.5, c) 4.5, d) 5.6, e) 6.4 and f) 8.0. A and B represent the two isomers observed for species $[Al_2L_2H_{-n}]$, while M represents $[AlLH_{-3}]$ (see text).

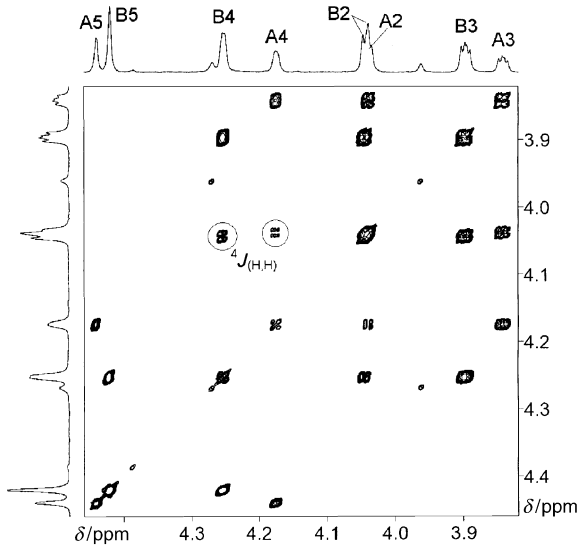


Figure 6. $^1$H-COSY spectrum recorded at pH 5.6 for a solution that contains $Al^{III}$ ions and mucic acid in a 1:1.1 ratio. The spectrum shows the $^4J_{H,H}$ coupling between H2 and H4.

and heterocorrelated $^1$H–$^{13}$C measurements (see Figure S3 in the Supporting Information), the scalar and dipolar connections allowed species A and B to be unambiguously distinguished. The absence of exchange peaks in phase with the diagonal in the phase-sensitive NOESY spectrum indicates that chemical exchange between these species, if any, must be extremely slow.[15] A complete list of the $^1$H and $^{13}$C NMR resonances is reported in Table 2. The $^1$H NMR signals for the most abundant species at 4.419 and 4.039 ppm were assigned to H5 and H2 because they are connected with the carbonyl carbons at $\delta$ 184.80 and 188.41 ppm, respectively. As the two ends of mucic acid are magnetically equivalent, the NMR signals for the complexes were numbered arbitrarily. To facilitate comparisons with the spectra for the saccharic acid complexes, the doublet at 4.478 ppm with a coupling constant of $^3J_{(H,H)} = 0.98$ Hz was denoted as H5. Such a low value for $^3J_{(H,H)}$ again suggests a dihedral angle close to 90° for these species. Similar features are observed for the signals of the less abundant species. These spectra are peculiar in that in the $^1$H-COSY spectrum (Figure 6), a $^4J_{(H,H)}$ coupling constant is observed between H2 and H4 for both isomers. Therefore, in contrast with what was found for the $Al^{III}$/saccharic acid system, mucic acid seems to coordinate to the $Al^{III}$ ion to afford two isomers of the dimeric species $[Al_2L_2H_{-4}]^{2-}$. Since four resonances of similar shape have been detected in the $^1$H NMR spectrum for both isomers, we argue that the ligands are coordinated to the metal ions in a similar manner. However, the two ends of each ligand are bound differently, therefore the magnetic equivalence of the nuclei observed in free mucic acid is destroyed.

At lower pH values, as in the case of saccharic acid, the two signal groups are shifted downfield, because of fast proton-exchange reactions between the differently protonated dimeric species. However, their relative intensities remain practically unchanged. Below pH 3, apart from the signals that arise from the free ligand and the dimeric complexes, resonances attributable to mononuclear complexes are also detected.

At pH > 7.5, new resonances (M) that belong to species such as $[AlLH_{-3}]^{2-}$ are observed (see Figure 5f). Again, the shapes of the signals in the NMR spectra indicate that the two ends of each ligand are bound differently (one is probably bound, while the other one is not). The proposed binding mode is ($COO^-$,$O^-$,$O^-$,$OH^-$).

**ESI-MS results**: ESI-MS measurements were carried out to prove the presence of dimeric species. The spectrum (Figure 7) recorded for a solution that contains $3\times10^{-4}$ M $Al^{III}$ ions and saccharic acid at pH 6.2 shows the presence of five species. Four of them were assigned as follows: $[Al_2L_2H_{-4}]^{2-}$ at $m/z$ 233 as well as its protonated and metallated forms $[Al_2L_2H_{-3}]^-$ at $m/z$ 467, $[NaAl_2L_2H_{-4}]^-$ at $m/z$ 489 and $[KAl_2L_2H_{-4}]^-$ at $m/z$ 505. The isotope pattern for the species at $m/z$ 233 presented in the inset zoom scan in Figure 7 was characteristic of a doubly-charged ion, and thus proved the dimeric character of the complex. MS/MS experiments confirmed that the fifth signal at $m/z$ 449 is the result of the $[Al_2L_2H_{-3}]^-$ complex undergoing fragmentation (loss of $H_2O$) in the ESI source. The presence of a signal at $m/z$ 467 raises the question of whether the species $[Al_2L_2H_{-3}]^-$ actually exists in the original solution or whether it is solely a product of the ESI process. Both potentiometry and NMR spectroscopy indicate the presence of a single species at pH 6, namely $[Al_2L_2H_{-4}]^{2-}$ (vide supra). Moreover, articles that deal with the description of inorganic

  

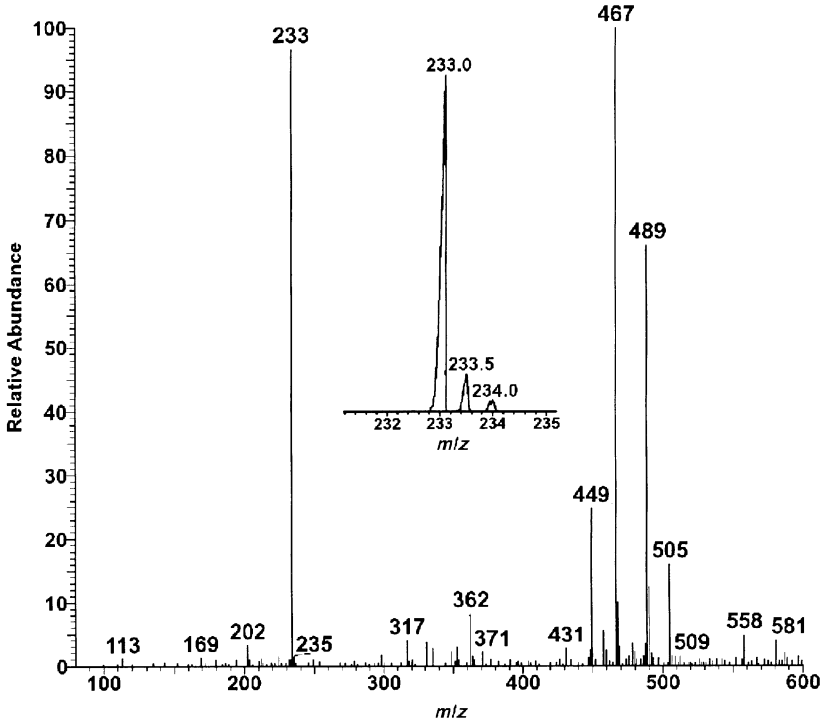


Figure 7. ESI-MS spectra for the $Al^{III}$/D-saccharic acid 1:1 ratio system at pH 6.2 ($c_{Al^{III}} = c_{ligand} = 0.3$ mM).

complex formation in aqueous solutions by the use of ESI-MS show that protonation and/or metallation of negatively charged complex ions can occur when they enter the gas phase.[16] Thus, we suggest that $[Al_2L_2H_{-3}]^-$, as well as $[NaAl_2L_2H_{-4}]^-$ and $[KAl_2L_2H_{-4}]^{2-}$ are formed during the ESI measurements.(Figure 7)

In the spectrum recorded at pH 3.5, only the signals for $[Al_2L_2H_{-3}]^-$ at *m/z* 467 and $[KAl_2L_2H_{-4}]^{2-}$ at *m/z* 505 can be observed. There is no evidence for the formation of monomeric complexes at lower *m/z* values. This means that the NMR spectrum pattern at pH 3.5 discussed above can only be explained by the existence of two different coordination isomers.

It is noteworthy that the ESI-MS spectrum recorded for a solution that contains $3\times10^{-4}$ M $Al^{III}$ ions and mucic acid at pH 6.0 also reveals the presence of only one ionic species. A base peak at *m/z* 467 corresponds to the protonated dimeric complex $[Al_2L_2H_{-3}]^-$.

From these experiments, ESI-MS unambiguously shows that dimeric complexes are formed preferentially, even in solutions ten times more dilute than the solutions used for the potentiometric measurements.

**The X-ray structure of $K_2[\{Al(C_6H_6O_8)(H_2O)\}_2]\cdot H_2O$ (1)**: Prismatic white crystals of **1**, which crystallised in the acentric space group $C222_1$, were obtained from aqueous solution. The absolute configuration of the crystals was determined through refinement methods. The molecular structure of the $[\{Al(C_6H_6O_8)(H_2O)\}_2]^{2-}$ ion along with the atom numbering is shown in Figure 8. The most relevant geometrical parameters are reported in Table S1 in the Supporting Information.

The structure in Figure 8 corresponds to the chemical formula of a dimerised $Al^{III}$ carboxyalcoholate. The deprotonated OH groups chelated to the $Al^{III}$ ion are in the $\alpha$ and $\alpha'$ (2 and 5) positions in the complexed carbohydrate acid, and the optically active saccharic acid has the D configuration (see Figure 1). The structure reported in Figure 8 is congruent with that given in Figure 1.

The molecular parameters indicate a distorted octahedral geometry around the $Al^{III}$ ion. The Al–O distances fall in the range $1.90\pm0.03$ Å. The exception is the Al–O6 distance which is 1.794(2) Å, and is probably due to ring-closure constraints. The carbonyl and carboxyl oxygen atoms of the carboxylate groups are distinctly differentiated (C1–O8 1.240(6), C1–O7 1.273(6), C6–O2 1.293(5) and C6–O1 1.293(5) Å). All the other geometrical parameters seem to have usual values. The torsion and bond angles are those imposed by the closure requirements of the seven- and five-membered rings present in the molecule.

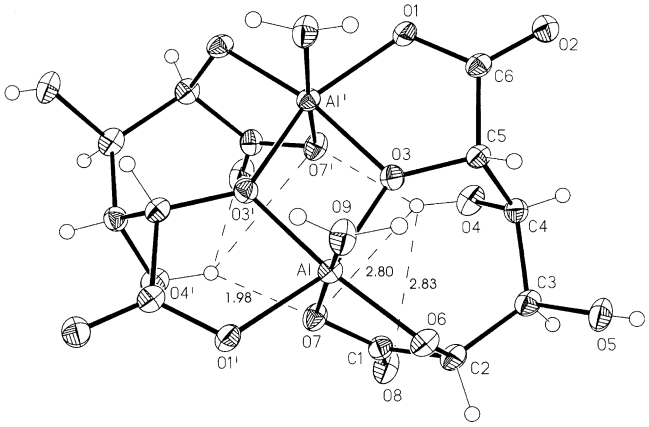


Figure 8. Perspective view of the anion $[Al(C_6H_6O_8)(H_2O)]_2^{2-}$ in which the atom labelling in Figure 1 is shown.

Dimerisation of the two complexed Al units is quite a common feature for $Al^{III}$ aqua-hydroxo ions.[17] In this case it is achieved through alcoholate oxygen bridges. Each Al atom is coordinated to two alcoholate (O6, O3) and one carboxylate (O7) group of the same molecular unit, to one alcoholate (O3′) and one carboxylate (O1′) group of the dimerised molecular unit, and to one water molecule (O9). Figure 9 schematically outlines the coordination mode in $[\{Al(C_6H_6O_8)(H_2O)\}_2]^{2-}$.

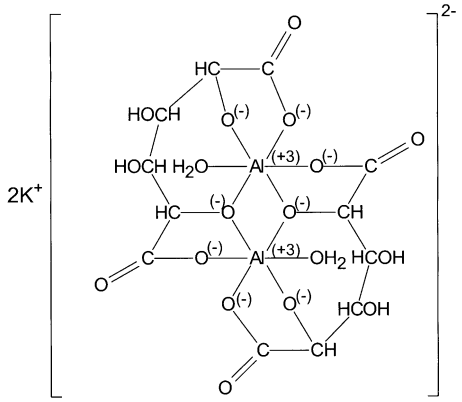


Figure 9. Schematic coordination mode of the complex anion $[Al(C_6H_6O_8)(H_2O)]_2^{2-}$.

The dimerised molecule is expected to be quite structurally stable. As usually occurs for aqua-hydroxides such as $[Al(H_2O)_5OH]^{2+}$ and other similar ions, a high equilibrium constant may be presumed for the dimerisation reaction $2[Al(C_6H_6O_8)(H_2O)]^- \rightleftharpoons [\{Al(C_6H_6O_8)(H_2O)\}_2]^{2-}$.[18] Moreover, in spite of the short intramolecular repulsive contact distances between the atoms in the apical positions (O7···O7′ 3.01(5), O9···O9′ 3.352(5) Å), strongly stabilizing hydrogen bonds (O4–H40···O7′ and O4′–H40′···O7 1.98 Å) and additional weaker hydrogen-bond interactions[19] (O4–H40···O7 and O4′–H40′···O7′ 2.80 Å) arise in the formed dimers. All of these interactions certainly favour dimerisation. For the hydrogen-bond lengths see Table S2 in the Supporting Information.

A projection of the packing mode of this ionic structure, as viewed down the *b* axis, is shown in Figure S4 in the Supporting Information (see also Figure 10).

The dimeric unit is centred on a twofold *z* axis. Both $K^+$ ions are located in special positions (K1 at *x*, $^1/_2$, $^1/_2$; K2 at $^1/_2$, *y*, $^3/_4$). The K1 cation lies at distances that range between 2.65–2.94 Å from seven oxygen atoms, including the water molecule of crystallisation, while K2 is surrounded by six oxygen atoms at distances in the range 2.78–2.92 Å. This roughly approximates a distorted capped trigonal prismatic and distorted trigonal prismatic coordination geometry, respectively[20] (see Table S2 and Figure S5 in the Supporting Information).

The hydration water molecule is at the non-coordinative distance of 3.36 Å from K2. An intricately thick network of intermolecular OH···O and CH···O hydrogen bonds (some are reported in Table S2) cooperate to provide further lattice stability.

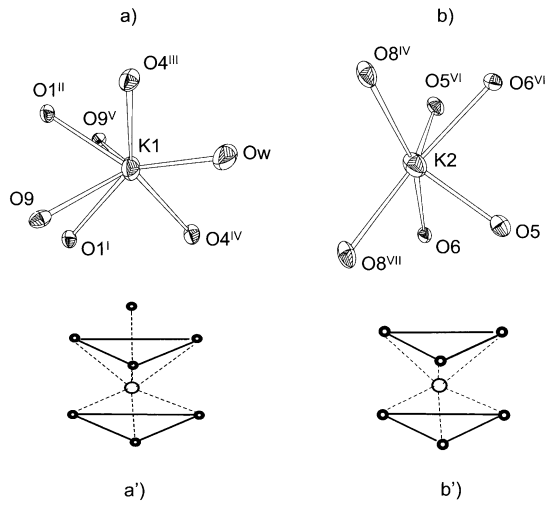


Figure 10. The actual coordination sphere around the $K^+$ ions (K1 and K2 in a and b, respectively) is reported and compared with the corresponding regular geometry (in a′ and b′, respectively).

**Theoretical calculations**: For a better understanding of the origin of the structural stability of the dimerised molecule, DFT calculations were performed on the molecular ion $[Al_2(C_6H_6O_8)_2(H_2O)_2]^{2-}$. Figure 11 displays the partial density of states (PDOS) of the bridged O3($O_\mu$) atoms (contributions of symmetry a and b are also included), together with the (Al–$O_\mu$) crystal orbital population (COOP). Analysis of the $O_\mu$ PDOS indicates that: 1) molecular orbitals (MOs) that are mainly localised on the $O_\mu$ 2p atomic orbitals (AOs) cover an energy range of about 9 eV (from −9.5 to −0.5 eV); and 2) they all lie well below the energy of the highest occupied MOs.[21] Moreover, despite several orbitals participating in the Al–$O_\mu$ interaction (17a, 18a, 22b, 32b, 33a, and 36a MOs), the strongest contributions to the

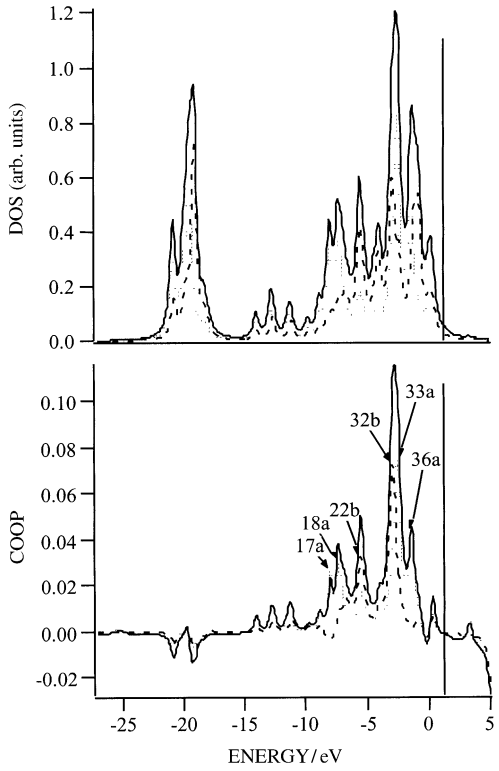


Figure 11. Top: PDOS of the μ-O atoms which have contributions of a and b symmetry (——=$O_\mu$, -----=$(O_\mu)^a$, – – –=$(O_\mu)^b$). Bottom: COOP between Al and μ-O atoms in which bonding (antibonding) states are represented by positive (negative) peaks. The vertical bar indicates the energy of the highest occupied MO (HOMO). ——=$(Al\text{-}O_\mu)^t$, -----=$(Al\text{-}O_\mu)^a$, – – –=$(Al\text{-}O_\mu)^b$.

  

$Al-O_{\mu}$ interaction are provided by the 32b, 33a, and 36a levels (see the corresponding COOP curves in Figure 11). Interestingly, the 32b and 33a MOs account for an in-plane σ interaction that involves, in the former case, both the Al 3s and Al 3p AOs, while in the latter case it is limited to the 3p AOs (see Figure S5 in the Supporting Information). On the other hand, the 36a MO orbital accounts for an out-of-plane π interaction which is delocalised over the four-membered ring (Figure S6 in the Supporting Information).

## Conclusions

The joint application of solution speciation, spectroscopic and solid-state X-ray diffraction methods, as well as theoretical calculations revealed that the terminal aldaric acid carboxylate groups behave as efficient anchors; they first bind the hard $Al^{III}$ metal ion, and then promote deprotonation and subsequent coordination of the weakly acidic alcoholic OH groups of these sugar derivatives.

At the beginning of complex formation ($pH < 3$), the ligands coordinate in a monodentate way to form lactate-like ($COO^-$,OH)-coordinated mononuclear complexes $[AlLH]^{2+}$, in which a protonated carboxylic group exists at the other end of the molecule. The metal-ion-induced deprotonation of the alcoholic OH functions at pH 3 may only occur in dinuclear complexes, as in the case of the structurally similar tartaric acid complexes.[6,7,9] Interestingly, even when the conformations of the molecules are identical, the two ends behave differently. This also applied in the case of mucic acid. The crystallographic structure of complex **1** reveals that the C5–$O^-$ group behaves as a bridging donor that coordinates to both $Al^{III}$ centres and forms a (5+7)-membered joint chelate ring system. On the other hand, the C2–$O^-$ donor binds to only one of the $Al^{III}$ centres in a lactate-like ($COO^-$,$O^-$) chelating mode. The octahedral $Al^{III}$ centres are arranged in a *cis* or parallel way, whereby the water molecules coordinate to the sixth coordination site on the same side of the complexes (see Figure 8). The ESI-MS and NMR studies confirm that complex **1** retains this dinuclear structure in solution. The rather rigid binding mode prevents coordination of the alcoholic functions in the $\beta$ position, but this may occur in the mononuclear complexes of aldonic acids.[10] The presence of the cyclic –Al–O–Al–O– core (see Figure 8) seems to be a peculiarity of the complexes for both saccharic acid and mucic acid. DFT calculations provide a rationale for the stability of this core in the former case, and it appears reasonable that mucic acid has a more flexible conformation. Apart from the binding mode in which a *cis* or parallel arrangement of the two coordinated water molecules (B form) occurs, mucic acid can also adopt another isomeric binding mode in solution. Here the two water molecules occupy antiparallel *trans* positions (A form). Formation of this last isomer in the $[Al_2L_2H_{-4}]^{2-}$ complex is not possible with saccharic acid for steric reasons. As the pH decreases the complex is protonated ($\log K$ values 2.85–4.05, see Table 1), and this protonation should occur on one of the alcoholate functions. The topmost line occupied MOs are mainly localised on O2 and O6; this strongly suggests that the protonation reaction involves these two oxygens. The protonation of O2 should not affect the structure of the molecular ion. However, formation of an OH bond with O6 would certainly weaken the O6–Al bond and make that end of the molecule more flexible for both saccharic and mucic acid. As a result, they should be able to adopt both conformations (A and B forms). This internal rearrangement of the isomers is slow on the $^1H$ and $^{13}C$ NMR timescales. Therefore, separate proton and carbon signals may be observed for each of the isomers (see Figures 4 and 5, and Figure S3 in the Supporting Information). It should be noted that the –Al–O–Al–O– core is retained during these stepwise deprotonations and seems to only be disrupted at $pH < 3$.

The $OH^-$ competition for the $Al^{III}$ ion increases at basic pH, and destroys the stable cyclic arrangement. As a result, a mononuclear complex $[AlLH_{-3}]^{2-}$ with a ($COO^-$,$O^-$,$O^-$,$OH^-$) coordination is initially formed (see Figure 2 and 3), but ultimately the ligand molecule is completely displaced from the coordination sphere of the metal ion by $OH^-$ to give the very stable hydroxo species $[Al(OH)_4]^-$.

This study has revealed that sugar derivatives which contain negatively charged O-donor moieties in close proximity to the alcoholic functions may be efficient and strong binders of metal ions in biological systems and may, therefore, play important roles in the transport, metabolism, and even biological functions of both carbohydrates and metal ions. The different sugar carboxylate conformations may finely tune their metal-binding abilities. In particular, the two aldaric acids investigated tended to form coordination isomers rather differently because of the differences in the rigidity of the stable –Al–O–Al–O– core.

## Experimental Section

**Reagents**: D-Saccharic acid potassium salt and mucic acid of the highest analytical purity (Sigma products) were used without further purification. Stock solutions of the ligands had a basic pH to avoid lactonisation, and were prepared freshly every day. The exact concentrations of the ligand solutions were determined by potentiometric titration by using the Gran method.[22] The $Al^{III}$ ion stock solution was prepared from recrystallised $AlCl_3 \cdot 6H_2O$, and its metal-ion concentration was determined gravimetrically from its oxinate. The stock solution contained 0.1 M HCl to prevent hydrolysis of the metal ion.

**Potentiometric measurements**: The stability constants for the proton and $Al^{III}$ ion ligand complexes were determined by pH potentiometric titrations of 25 mL samples. The ligand concentration was 0.004 M (with a metal-ion/ligand ratio of 0:4, 1:4, 2:4, or 4:4), 0.002 M (with a metal-ion/ligand ratio of 0:2 or 1:2), and 0.001 M (with a metal-ion/ligand ratio of 0:1, 1:1, or 0.5:1). The more dilute concentrations contained the mucic acid system because of its lower solubility. The pH range studied was 2–10. The titrations were performed with a 0.2 M carbonate-free KOH solution of known concentration under a purified argon atmosphere. The ionic strength of all solutions was adjusted to 0.2 M KCl and the samples were thermostatted at 25.0 ± 0.1 °C. Duplicate titrations were performed. The reproducibility of the titrations was within 0.005 of a pH unit. Titration points obtained when a pH equilibrium was not attained within 5 min were omitted from the evaluation. The pH was measured with a Radiometer PHM 84 instrument with a CMAWL Russel combined glass electrode; this was calibrated for hydrogen-ion concentration according to Irving et al.[23] The concentration stability constants $\beta_{pqr} = [M_pL_qH_r]/$

$[M]^p[L]^q[H]^r$ were calculated with the aid of the computer program PSEQUAD.[24] The stability constants used for the hydroxo species of the $Al^{III}$ ion were taken from reference [25] and corrected to $I=0.2$ M by using the Davies equation (−5.49 for $[AlH_{-1}]^{2+}$, −13.54 for $[Al_3H_{-4}]^{5+}$, −108.62 for $[Al_{13}H_{-32}]^{7+}$ and −23.40 for $[AlH_{-4}]^{-}$).

**Preparation of $K_2[\{Al(C_6H_6O_8)(H_2O)\}_2]\cdot H_2O$ (1)**: A mixture of $AlCl_3\cdot 6H_2O$ (0.241 g, 1 mmol) and D-saccharic acid potassium salt (0.252 g, 1.02 mmol) was dissolved in distilled water (10 mL). The pH of the solution was adjusted with KOH to about 6.2. Addition of absolute ethanol (ca. 30 mL) yielded a microcrystalline powder. This was isolated by filtration and dried under vacuum at 30 °C for 12 h; yield: 0.16 g (55.17 %). Crystals suitable for X-ray diffraction studies were obtained by dissolving the microcrystalline powder (0.107 g) in water (1.5 mL), adding ethanol, and leaving this solution to stand at room temperature. FTIR (KBr): $\tilde{\nu}_{COO}=1646\ cm^{-1}$; elemental analysis calcd (%) for $K_2[Al(C_6H_6O_8)(H_2O)]_2\cdot H_2O$: C 24.08, H 3.01; found: C 22.86, H 2.79.

**NMR spectroscopy**: $^1H$ NMR (400.13 MHz), $^{13}C$ NMR (100.61 MHz) and two-dimensional spectra (100.61 MHz) were recorded at 25 °C on a Bruker Avance DRX-400 spectrometer equipped with a VSP-400 reverse detector broad-band probe and a Bruker VST-100 temperature controller. The pH dependent spectra were measured at 25 °C on a Bruker AC-200 instrument. Chemical shifts were referenced to the signal of DSS (DSS = 2,2-dimethyl-2-silapentane-5-sulfonate) as an internal standard. The samples were prepared in $D_2O$ and the pH was adjusted with concentrated NaOD and DCl by using the relationship pH = pD + 0.4. The concentrations of the solutions were 0.004–0.08 M with respect to the $Al^{III}$ ion and the metal-ion/ligand ratio was 1:1 or 1:3.

Presaturation of the $H_2O$ signal was performed when necessary. Suitable integral values for the proton spectra were obtained with a prescan delay of 10 s. The proton resonances were assigned by means of standard chemical shift correlations, as well as COSY, TOCSY, and NOESY experiments. The $^{13}C$ NMR resonances were assigned through 2D-heterocorrelated COSY experiments (HMQC with the bird sequence[26] and quadrature along F1 was achieved by using the TPPI (TPPI = time-proportional phase incrementation) method[27] for the hydrogen-bonded carbon atoms and HMBC[28] for the quaternary ones). For atom labelling see Figure 1, as well as Table 2.

**ESI-MS measurements**: The mass spectrometry measurements were recorded on an LCQ (ThermoFinnigan) mass spectrometer equipped with an electrospray ion source. MS and multiple mass spectrometry ($MS^n$) experiments were performed in the negative ion mode by direct infusion of an aqueous solution of the analyte at a flow rate of 5 $\mu L\,min^{-1}$.[29] Collisional experiments on preselected ion species were performed by application of a supplementary rf (rf = radio frequency) voltage in the range 0–5 V with helium as a target gas.

The samples were prepared in distilled water. The concentration of the solutions was $3\times10^{-4}$ M with respect to the $Al^{III}$ ion at a metal-ion/ligand ratio of 1:1. The pH of the solutions was set at 3.5 or 6.2 with concentrated NaOH.

**X-ray structure determination**: A single prismatic (colourless) crystal with dimensions $0.32\times0.30\times0.24$ mm was lodged in a Lindemann glass capillary and centered on a four-circle Philips PW1100 (Febo System) diffractometer with graphite-monochromated $Mo_{K\alpha}$ radiation ($\lambda=0.71073$ Å). The orientation matrix and cell dimensions were determined by least-squares refinement of the angular positions of 30 reflections. Data were collected at room temperature. Three standard reflections were monitored for every 200 reflections. There were no significant fluctuations of intensities other than those expected from Poisson statistics. The intensity data were corrected for Lorentz polarisation effects and for absorption as described by North et al.[30]

The structure was solved by direct methods.[31] Refinement was carried out by full-matrix least-squares. The function minimised was $\Sigma w(F_o^2-F_c^2)^2$ with the weighting scheme $w=1/[\sigma^2(F_o^2)+(0.1090\,P)^2+3.82\,P]$ where $P=\max(F_o^2+2F_c^2)/3$. All non-hydrogen atoms were refined with anisotropic thermal parameters. The H atoms, except those of the non-coordinated water molecule, were located and refined isotropically. The conventional $R=0.059$ was based on $F$ values of 1304 reflections that had $F_o^2\geq2\sigma(F_o)^2$ and $S=1.14$ ($wR$ on $F^2=0.150$). The absolute configuration determination was based on calculations by Flack.[32] Structure refinement was carried out with SHELXL-97[33] with the scattering factors enclosed therein. Drawings were produced using ORTEP II.[34] Crystallographic data are listed in Table 3.

CCDC-208181 contains the supplementary crystallographic data for this paper. These data can be obtained free of charge via www.ccdc.cam.ac.uk/conts/retrieving.html (or from the Cambridge Crystallographic Data Centre, 12 Union Road, Cambridge CB2 1EZ, UK; fax: (+44) 1223-336-033; or e-mail: deposit@ccdc.cam.ac.uk).

**Computational details**: The calculations reported herein were carried out in accordance with DFT with the ADF package[35] developed by Baerends et al.[36] A triple-ζ Slater-type basis set was used for the Al atoms, while a double-ζ basis was used for O, C, and H valence orbitals. The inner-core shells [Al(1s2s2p), O(1s), and C(1s)] were treated according to the frozen-core approximation. Non-local corrections to the LDA (LDA = local density approximation) functional were self-consistently included by adopting the Becke[37a] and Perdow[37b,c] functionals for the exchange and correlation parts, respectively. The atomic positions in $[Al_2(C_6H_6O_8)_2(H_2O)_2]^{2-}$ were determined by referring to X-ray crystal data included here and idealised to the $C_2$ symmetry (see Figure 8). Information concerning the disposition and composition of energy levels over a broad range of energies was obtained through total and partial density of states (DOS and PDOS, respectively).[38] The bonding character of selected molecular orbitals was assessed by means of COOP curves[38] and 2D contour plots. Both PDOS and COOP curves were computed by weighting one-electron energy levels with their basis orbital percentage and applying a Lorentzian broadening factor of 0.25 eV.

## Acknowledgement

This work was carried out in the frame of a CNR–MTA bilateral cooperation Scheme (Project I180) and was supported by the National Research Fund of Hungary (OTKA T038560).

[1] *Metal Ions in Biological Systems, Vol. 24* (Ed.: H. Sigel), Marcel Dekker, New York, **1988**, and references therein.
[2] *Aluminium and Alzheimer*'s *Disease* (Ed.: C. Exley), Elsevier, Amsterdam, **2001**, and references therein.
[3] T. Kiss, E. Farkas, *Perspect. Bioinorg. Chem.* **1996**, *3*, 199–250.
[4] a) L. O. Öhman, S. Sjöberg, *J. Chem. Soc. Dalton Trans.* **1983**, 2513–2517; b) L. O. Öhman, *Inorg. Chem.* **1988**, *27*, 2565–2570.
[5] A. Lakatos, I. Bányai, P. Decock, T. Kiss, *Eur. J. Inorg. Chem.* **2001**, 461–469.
[6] F. R. Venema, J. A. Peters, H. van Bekkum, *Inorg. Chim. Acta* **1992**, *191*, 261–270.
[7] E. Marklund, L. O. Öhman, *J. Chem. Soc. Dalton Trans.* **1990**, 755–760.
[8] R. J. Motekaitis, A. E. Martell, *Inorg. Chem.* **1984**, *23*, 18–23.
[9] F. R. Venema, J. A. Peters, H. van Bekkum, *Recl. Trav. Chim. Pays-Bas* **1993**, *112*, 445–450.
[10] B. Gyurcsik, L. Nagy, *Coord. Chem. Rev.* **2000**, *203*, 81–149.
[11] J. G. Velasco, J. Ortega, J. Sancho, *J. Inorg. Nucl. Chem.* **1976**, *38*, 889–895.
[12] E. Bottari, *Monatsh. Chem.* **1968**, *99*, 176–186.
[13] M. van Duin, J. A. Peters, A. P. G. Kieboom, H. van Bekkum, *Magn. Reson. Chem.* **1986**, *24*, 832–833.
[14] H. Gunther, *NMR Spectroscopy*, Wiley, New York, **1980**, pp. 106–107.
[15] C. L. Perrin, T. J. Dwyer, *Chem. Rev.* **1990**, *90*, 935–967.
[16] M. J. Deery, T. Fernandez, O. W. Howarth, K. R. Jennings, *J. Chem. Soc. Dalton Trans.* **1988**, 2177–2183.
[17] a) J. W. Akitt, J. M. Elders, *J. Chem. Soc. Faraday Trans. 1* **1985**, *1*, 1923–1930; b) J. W. Akitt, J. M. Elders, *Bull. Soc. Chim. Fr.* **1986**, 10–16.
[18] J. W. Akitt, *J. Chem. Soc. Dalton Trans.* **1984**, 981–984.
[19] a) G. A. Jeffrey, W. Saenger, *Hydrogen Bonding in Biological Structures*, Springen, Berlin, **1991**; b) R. Taylor, O. Kenard, *J. Am. Chem. Soc.* **1982**, *104*, 5063–5070.
[20] D. L. Kepert, *Prog. Inorg. Chem.* **1979**, *25*, 41–144.

  

[21] Both the 45a and 45b orbitals, HOMOs of symmetry a and b, respectively, have a negligible localisation on the $O_\mu$ AOs.
[22] G. Gran, *Acta Chem. Scand.* **1950**, *4*, 559–575.
[23] H. M. Irving, M. G. Miles, L. D. Pettit, *Anal. Chim. Acta* **1967**, *38*, 475–481.
[24] L. Zékány, I. Nagypál, G. Peintler, *PSEQUAD for Chemical Equilibria*, Technical Software Distribution, Baltimore, **1991**.
[25] L. O. Öhman, S. Sjöberg, *Acta Chem. Scand.* **1982** *36*, 47–53.
[26] A. Bax and S. Subramian, *J. Magn. Reson.* **1986**, *67*, 565–569.
[27] a) G. Otting, K. Wüthrich, *J. Magn. Reson.* **1988**, *76*, 569–571; b) G. Drobny, A. Pines, S. Sinton, D. P. Weitekamp, D. Wemmer, *Faraday Symp. Chem. Soc.* **1978**, *13*, 49–55.
[28] A. Bax, M. F. Summers, *J. Am. Chem. Soc.* **1986**, *108*, 2093–2094.
[29] a) S. A. Hofstadler, R. Bakhtiar, R. D. Smith, *J. Chem. Educ.* **1996**, *73*, A82; b) S. A. Hofstadler, R. Bakhtiar, R. D. Smith, *J. Chem. Educ.* **1996**, *73*, A118; c) L. A. P. Kane-Maguire, R. Kanitz, M. M. Sheil, *J. Organomet. Chem.* **1995**, *486*, 243–248.
[30] A. C. T. North, D. C. Philips, F. S. Mathews, *Acta Crystallogr. Sect. A* **1968**, *24*, 351–359.
[31] A. Altomare, G. Cascarano, C. Giacovazzo, A. Guagliardi, M. C. Burla, G. Polidori, M. Camalli, *J. Appl. Crystallogr.* **1994**, *27*, 435.
[32] H. D. Flack, *Acta Crystallogr. Sect. A* **1983**, *39*, 876–881.
[33] G. M. Sheldrick, SHELXL-97, Program for the Refinement of Crystal Structure, University of Göttingen (Germany), **1996**.
[34] C. K. Johnson, ORTEP II report ORNL-5138, Oak Ridge National Laboratory, Tennesse (USA), **1976**.
[35] ADF 1999, Dept. of Theoretical Chemistry, Vrije Universiteit, Amsterdam, **1999**.
[36] a) D. Post, E. J. Baerends, *J. Chem. Phys.* **1983**, *78*, 5663; b) E. J. Baerends, D. E. Ellis, P. Ros, *J. Chem. Phys.* **1973**, *2*, 41–51.
[37] a) A. Becke, *Phys. Rev. A* **1988**, *38*, 3098; b) J. P. Perdew, *Phys. Rev. B* **1986**, *33*, 8822; c) J. P. Perdew, *Phys. Rev. B* **1986**, *34*, 7406.
[38] R. Hoffmann, *Solids and Surfaces: A Chemist*'s *View of Bonding in Extended Structures*, VCH, New York, **1988.**

Received: July 11, 2003
Revised: October 7, 2003 [F5328]